Engineering a Synthetic Extra-Cellular Matrix for *In Vitro* Cartilage Tissue Production

Gwen E. Owens

Thesis Submitted to the

Biology Department of Cornell University

In Partial Fulfillment of the Honors Requirement for the Degree of

Bachelors of Science

Dr. Lawrence Bonassar

Research Advisor

May 15, 2007

Ithaca, NY

Abstract

Engineering a Synthetic Extra-Cellular Matrix for

***In Vitro* Cartilage Tissue Production**

In this study, growth factor binding found in natural extra-cellular matrix (ECM) was mimicked by a modified polymer scaffold that could attract either Insulin-Like Growth Factor-I (IGF-I), a growth factor known to stimulate ECM production by chondrocytes, and Transforming Growth Factor-β1 (TGF-β1), a growth factor known to induce chondrogenesis in mesenchymal stem cells.

Short growth factor-binding peptides were synthesized and covalently attached to an alginate polymer scaffold. Using self-assembled monolayer (SAM) chemistry, these modified alginate layers were characterized using Imaging Ellipsometry (IE). Affinity of each growth factor for its respective synthetic peptide was quantified via Surface Plasmon Resonance (SPR). The density of binding peptides bound to alginate was determined using Attenuated Total Reflectance Fourier Transform Infrared Spectroscopy (ATR-FTIR). Computational diffusion modeling was used to design an ELISA-based diffusion experiment. Mesenchymal stem cells and chondrocytes were grown in chemically modified-alginate beads with and without added growth factor; modification increased ECM production in both kinds of cells. Thus, through this novel system of peptide-modified alginate scaffolds, growth factors were specifically but non-covalently retained by alginate, allowing for controlled release of growth factors.

Loss or failure of an organ or tissue is one of the most frequent and costly problems in human health care. Yearly, more than one million surgical procedures in the United States involve the replacement of bone or cartilage, including more than 500,000 arthroplastic procedures and total joint replacements.[1, 2] Degenerative diseases such as osteoarthritis are the major cause of loss of cartilage. Osteoarthritis alone affects more than 10% of Americans older than 60 years.[3] Trauma to intervertebral disk and meniscus cartilage are primary sources of cartilage damage in younger patients.[4] Additionally, reconstruction of craniofacial defects such as cleft palate[5] or microtia[6] often require the use of cartilage transplantation.

1.1 Cartilage structure & composition

There are four primary types of cartilage, each distinguished by specific cellular components and functions: hyaline cartilage, costochondral cartilage, elastic cartilage, and fibrocartilage.[4]

Hyaline	**Costochondral**	**Elastic**	**Fibrocartilage**
Articular joints	Rib	Ear	Tendon insertion site
Nose	Growth plate		Ligament insertion site
Trachea			Meniscus
Intervertebral disk (NP)			Intervertebral disk (AP)
Vertebral end plate			

Table 1.1. Summary of mammalian cartilage types and locations.[4]

The composition of the extracellular matrix (ECM) that surrounds chondrocytes *in vivo* determines the functional behavior of cartilage. For hyaline cartilage, the ECM generally is composed of 50% fibrous matrix (including collagens II, IX, and IX, as well as occasional elastic fibers) and 50% ground substance, including proteoglycans and non-collagenous proteins.[7] Collagens play a key role in the matrix structure of the ECM, as the collagen fiber triple-helices are strong in tension and resist osmotic pressure created by surround ECM material. Proteoglycans are composed of glycosaminoglycan (GAG) carbohydrate chains covalently bound to a protein core. Aggrecan is the largest proteoglycan, and is a key component in distributing load in weight-bearing joints. Other proteins include decorin, a small proteoglycan that has been shown to bind to growth factors,[8] and hyaluronic acid, which acts as a backbone to which aggrecan

molecules bind to form aggregates. These macromolecular components are chemically and mechanically connected to form a continuous three-dimensional network.

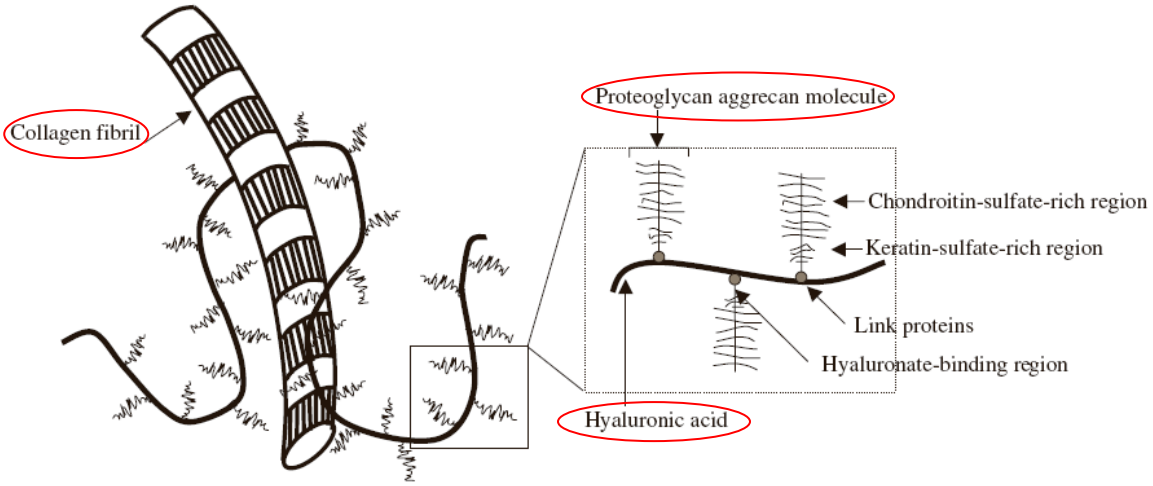

Figure 1.1 Summary of macromolecular constituents of cartilage ECM. The ECM is composed of proteoglycans attached to a backbone of hyaluronic acids that is intertwined among collagen fibrils. From Moreland.[9]

1.2 Cartilage repair methods

Loss of or damage to cartilage tissue is particularly problematic because cartilage has very limited potential to spontaneously heal. Adult articular cartilage is avascular, aneural, and contains no lymphatic drainage; in fact, articular cartilage defects larger than 4 mm in diameter rarely regenerate.[10]

Surgical interventions to repair cartilage are listed in Table 1.2. Unfortunately, no method has been shown to create superior quality articular cartilage repair tissue. Arthroscopic lavage and debridement do not induce repair of cartilage tissue, but rather provide temporary relief of osteoarthritis symptoms. Bone marrow stimulation produces primarily fibrocartilage, which due to structural properties different from articular cartilage, does not offer a long-term cure. Soft tissue grafts can produce repair tissue that is similar to hyaline cartilage, but the technique is limited by tissue graft availability and a tendency toward ossification of repair tissue.

Surgical Technique	Method
Arthroscopic Lavage & Debridement	Damaged articular cartilage tissue is rinsed or removed
Bone Marrow Stimulation *Pridie Drilling* *Abrasion arthroplasty* *Microfracture*	Subchondral bone marrow underlying regions of damaged articular cartilage is damaged to stimulate a repair reaction[11]
Soft tissue grafts	Periosteum or perichondrium are transplanted to full thickness defects of articular cartilage
Autologous Cartilage Tissue Transplantation	Healthy cartilage is excised, chondrocytes are expanded in culture and reinjected into articular cartilage defect

Table 1.2. Summary of current surgical techniques to repair cartilage defects.

Adapted from Gilbert[12] and Minas et al.[13]

In 1994, Brittenberg et al[2] successfully reported autologous chondrocyte implantation using a monolayer culture system to treat cartilage defects. In autologous cartilage tissue transplantation, a healthy biopsy is excised from a non-load-bearing region of articular cartilage. The chondrocytes are released by enzymatic digestion and expanded in culture. After the defect has been sutured, the cultured autologous chondrocytes are injected into the defect site.[14] In the United States and Europe, similar cell processing has been conducted on a commercial basis.

However, autologous tissue transplantation has several disadvantages, including reacquisition of phenotypes of dedifferentiated chondrocytes and uneven distribution of transplanted chondrocytes.[15] Additional difficulties have been encountered due to scarcity of donor sites, cell death during harvest, and difficulties integrating transplanted cartilage into the implant site. In response to a growing demand for cartilage tissue replacements, engineered cartilage tissues have thus been proposed as a method to repair or replace injured or diseased cartilage.

1.3 Matrix materials & synthetic scaffolds

Synthetic ECMs, or tissue scaffolds, are being used to replace many structural functions of the native ECM. These engineered ECMs provide mechanical integrity to new cartilage tissue, organize cells into a stable three-dimensional architecture, and provide a hydrated space for the diffusion of nutrients and metabolites to and from the cells. As in autologous tissue transplantation, cells are removed from the body, grown in culture, applied to the synthetic scaffold material *in vitro*, and then transplanted. The cells in the scaffold should then produce ECM components *in vivo,* which resemble native cartilage as closely as possible in its functional and morphological properties.

However, one key difficulty in production of synthetic cartilage tissue in artificial scaffolds is significant loss of regulatory proteins after initial transplantation, which are essential components for tissue development and proliferation. Cell signaling through bound ECM molecules is a requirement for survival of most cell types; cell signaling orchestrates critical roles in many cellular functions including migration, proliferation, differentiation, and apoptosis.[7] Due to reduction of cellular interaction with natural ECM proteins, researchers have not yet produced mechanically functional, clinically useful tissue that can match tissues produced under normal physiological conditions using either transplanted chondrocytes (cartilage producing cells) or mesenchymal stem cells (chondrocytes progenitor cells).

Most strategies for tissue engineering are based on the use of biodegradable polymers as temporary scaffold materials for differentiated chondrocytes or mesenchymal stem cells. Various hydrogels have been used as synthetic ECMs for cell immobilization, transplantation, and tissue engineering. Alginates are naturally derived polysaccharides that have been extensively used as hydrogel synthetic ECMs. Alginate was chosen as the scaffolding material for this experiment because alginate polymers are regarded as an ideal synthetic matrix material, i.e., their interactions with cells are well characterized; they are amenable to sterilization and storage; and they may be chemically modified with

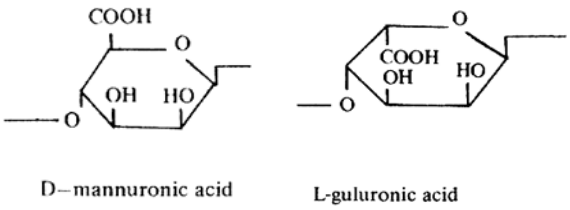

Figure 1.2. Molecular structure of alginate monomers

simple chemistries. Structurally, alginate is composed of (1-4)-linked β-D-mannuronic acid (M units) and α-L-guluronic acid (G units). The alginate molecule is a block copolymer composed of regions of sequential M units, regions of sequential G units, and regions of randomly organized M and G units.[16] However, due to its hydrophilic nature, alginate discourages protein adsorption. Therefore, mammalian cells are unable to interact specifically with alginate hydrogels.[17] Scaffolds utilizing hydrophobic materials may bind cells and proteins through physical adsorption; however, this is a poor substitute for natural ECM.

1.4 Growth factors

Our tissue engineering approach to cartilage repair involves not only cells and matrices, but also signaling molecules. In order to create structurally and functionally competent cartilage repair tissue, our primary interest was to create biomimetic binding proteins to bind two key growth factors that have well known effects on cartilage-producing cells. By non-covalently binding cell signaling proteins to alginate, a composite hydrogel composed of cells, bound growth factors, and alginate may allow for sustainable tissue growth and repair.

1.4.1 Insulin-Like Growth Factor-I

The first growth factor of interest, Insulin-Like Growth Factor-I (IGF-I), is a growth regulatory protein involved in stimulation of cellular proliferation, cartilage sulfonation, DNA synthesis, proteogylcan synthesis, and glycosaminoglycan synthesis; it is essential for normal mammalian growth and development.[18] IGF-I can also enhance cell-based repair of articular cartilage.[19] IGF-I is a single polypeptide chain of 70 amino acids that can be bound by one of six different insulin-like growth factor binding proteins (IGFBPs), which act as important regulators of IGF action.

Most of the IGF-I molecules in serum are found complexed with IGFBP-3.[20] To a lesser degree, IGFBP-5 also forms complexes with IGF-I.[21] An even smaller proportion of IGF-I is carried by other IGFBPs, and less than 1% of IGF-I circulates in the free (unbound) form.[20] All human IGFBPs contain between 216 and 289 amino acids organized into three domains of approximately equal size with conserved N-terminal and

C-terminal domains joined by a "linker" L-domain.[22] Both the N- and C-domains of IGFBPs participate in binding to IGF.

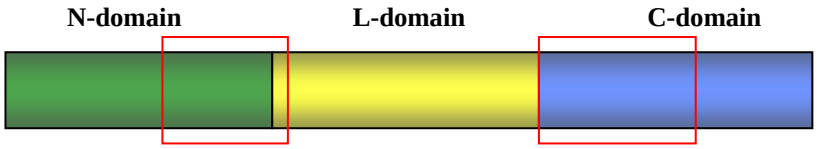

Figure 1.3. Structure of IGFBPs in three domains, each of which contributes to chemical binding properties. Regions of the N- and C-terminal domains involved in IGF binding are enclosed in red boxes. Adapted from Bach et al.[22]

During the last decade, several publications have reported an increasingly smaller N-domain fragment of IGFBP-5 that alone can bind IGF-I with only 10 to 1000 times lower affinity than the full length IGFBP-5. A critical 40-amino acid sequence derived from the N-domain region of IGFBP-5 was determined in 1998 by Kalus et al.[18, 23] Termed "Mini-BP-5," this sequence was shown to have a 37 nM affinity for IGF-I, compared to 3.7 nM for the entire binding protein, as determined by a surface plasmon resonance binding kinetics study. Another small segment, called "10 kDa IGFBP-5," was also analyzed; however, its binding was much less than the other analytes considered.

Analyte	**Ligand**	**k_{on} 10^6 / Ms**	**k_{off} 1 / s**	**K_D**
IGFBP-5	IGF-I	1.2	4.4E-03	3.7 nM
Mini-IGFBP-5	IGF-I	5.1	1.9E-01	37 nM
10 kDa IGFBP-5	IGF-I	1.9	3.0E-01	158 nM

Table 1.3. Binding affinity values for IGFBP-5 and small peptide sequences for IGF-I. Adapted from Kalus et al.[18, 23]

The greater affinity to the full IGFBP-5 is a result of more rapid dissociation of IGF-I from the N-terminal domain than from the full-length IGFBP-5. This mini-BP-5 sequence consists solely of a compact three-stranded β-sheet and a short α-helix, stabilized by two disulfide bonds.[22] The sequence alignment below

shows the location of mini-BP-5 within the IGFBP-5 molecule, as well as a smaller sequence, highlighted in yellow, upon which much of the work in this thesis is based.

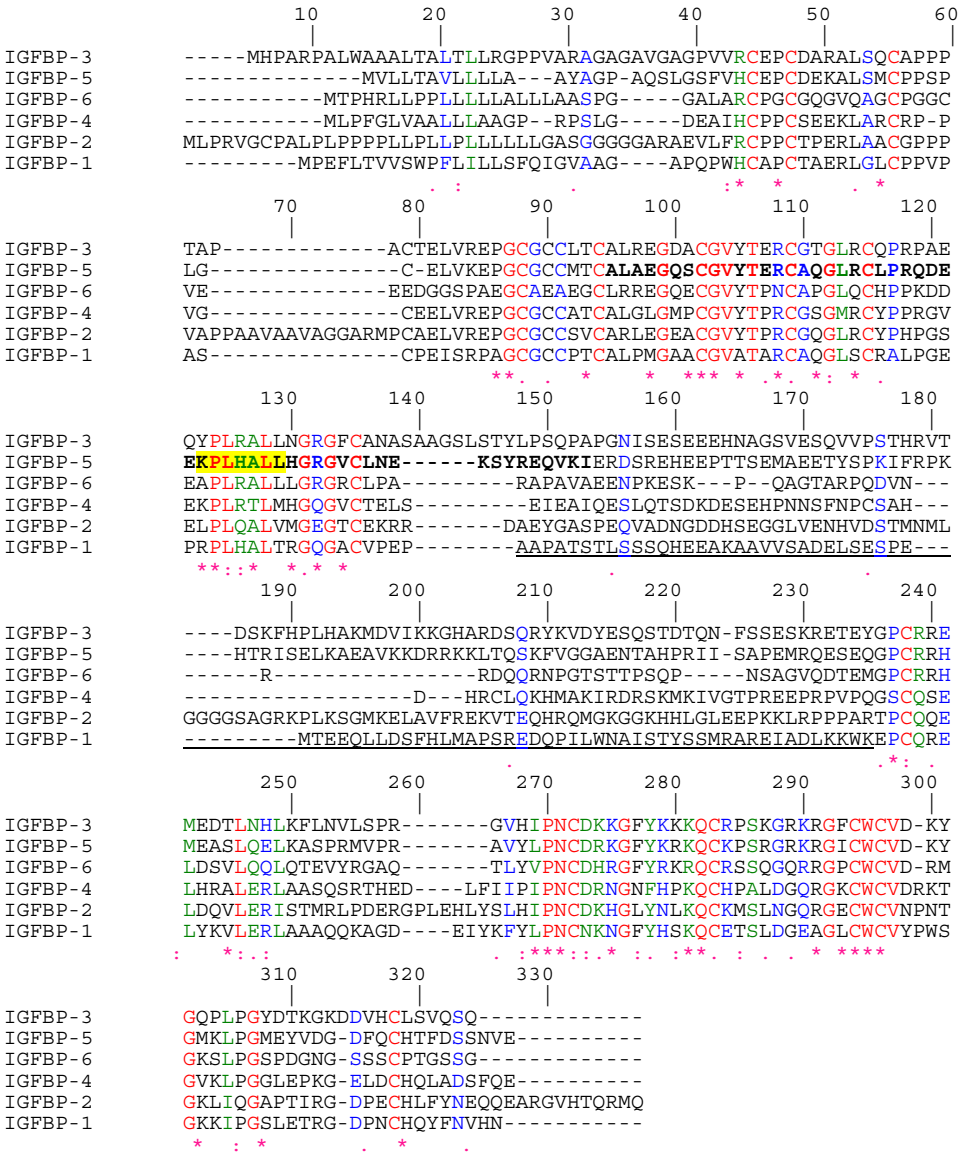

Figure 1.4. Sequence alignment of IGFBP-1 to -6 performed by the author using protein sequences from NCBI Entrex Protein; sequences aligned using CLUSTALW Network Protein Sequence Analysis.[24] Highly conserved residues are indicated by red shading. "Mini-BP-5" is bolded. Residues that were selected for this study are highlighted in yellow. The linker domain is underlined.

Because this and other studies have proposed that the N-terminal region of IGFBP-5 contains a hydrophobic binding pocket between residues 38 and 74 that is required for high-affinity binding, Imai et al. developed a site-directed mutagenesis study to determine the importance of several of the amino acids in this region. When residues Lys[68], Pro[69], Leu[70], Leu[73], and Leu[74] in IGFBP-5 were altered (changing the one charged residue, Lys [68], to a neutral one and the four hydrophobic residues to nonhydrophobic residues), affinity for IGF-I decreased by 1000-fold. Therefore, this specific group of hydrophobic amino acids within the N-terminal third of IGFBP-5 appears critical for high affinity binding of IGF-I.[25]

Below is shown the crystal structure of the IGF-I complexed with mini-BP-5. The sequence $K_{68}P_{69}L_{70}H_{71}A_{72}L_{73}L_{74}$ within mini-BP-5 interacts with IGF-I within 4 Å, the limit for electrostatic interactions. Based on this data, as well as previous studies, $K_{68}P_{69}L_{70}H_{71}A_{72}L_{73}L_{74}$ was chosen for this study as a putative short binding sequence for IGF-I.

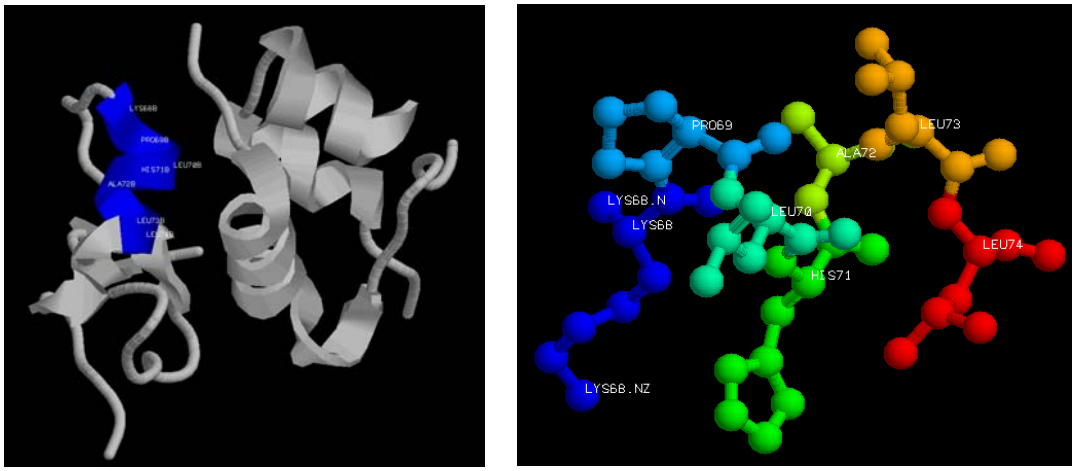

Figure 1.5. (Left) IGFBP-5 (left) bound to IGF-I (right). The binding sequence, KPLHALL, being tested in this study is labeled and highlighted in blue; (Right) Three-dimensional structure of KPLHALL.

1.4.2 Transforming Growth Factor-β1

The second growth factor of interest is transforming growth factor-beta (TGF-β1), another potent growth regulatory protein, that is involved in wound healing, growth and differentiation, angiogenesis, and

chondrogenesis of mesenchymal stem cells.[26] TGF-β1 is a disulfide-linked homodimer of two 112 amino acid polypeptides with a characteristic pattern of 9 cysteines. Recently, it has been found that thrombospondin-1 (TSP-1), a glycoprotein, is a key activator and regulator of TGF-β1 expression and signalling.[27-30] In 1995, Schultz-Cherry et al. found that the hexapeptide GGWSHW, derived from TSP-1, binds strongly to the sequence VLAL in active TGF-β1.[31, 32] Therefore, we have selected the amino acid sequence GGWSHW for study, as well as a control sequence GGASHA that was demonstrated by Murphy-Ullrich (unpublished data) to have no specific interaction with TGF-β1.

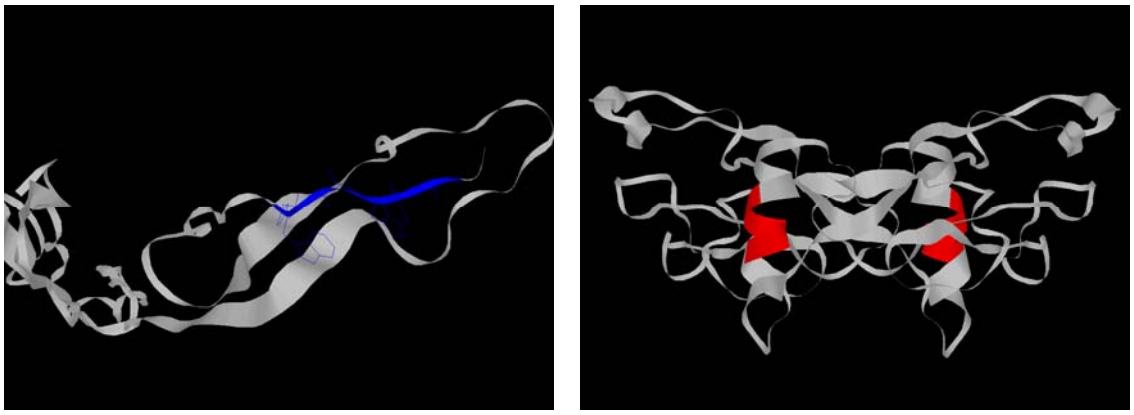

Figure 1.6. (Left) Crystal structure of thrombospondin-1, with the GGWSHW binding sequence highlighted in blue; (Right) Structure of TGF-β1, with the VLAL interaction sequence highlighted in red. Two binding sites are present as TGF-β1 is a homodimer.

1.5 Study Objectives

By using simple carbodiimide chemistry to attach these two short amino acid sequences from the binding areas of TSP-1 and IGFBP-5 to an alginate scaffold, it is hoped that growth factors will bind in a manner similar to that which occurs *in vivo* to improve the characteristics of engineered cartilage tissue. By non-covalently binding growth factors, we hope to be able to tailor specific cell-alginate interactions.

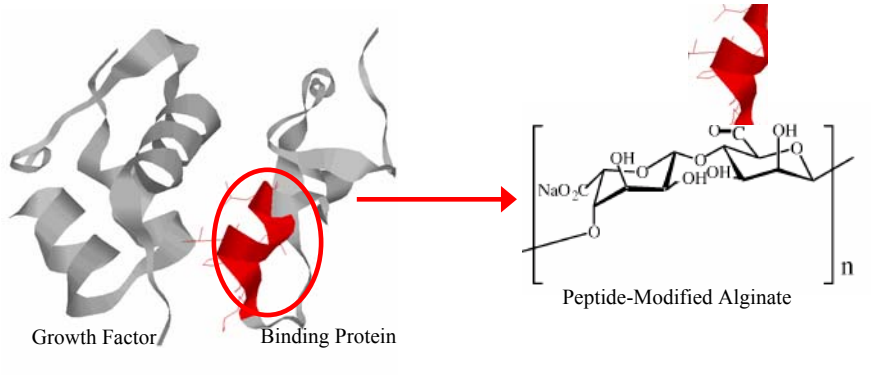

Figure 1.7. Project schematic; A short binding sequence (circled) from IGFBP-5 is covalently bound to alginate. This modified alginate attracts and non-covalently binds growth factors.

In order to characterize binding of IGF-I and TGF-β1 to an artificial ECM composed of peptide-modified sodium alginate, three studies were performed, each involving several different assays. This experiment began under the assumption that the sequences GGWSHW and KPLHALL bind to TGF-β1 and IGF-I, respectively, based on literature and sequence alignment studies performed by the author. The three studies include a binding kinetics study, in which the binding constants and characteristics of binding peptide-modified alginate on a molecular scale will be determined; a controlled-release study, in which the macromolecular diffusion and release properties of modified-alginate beads will be modeled and tested; and a cellular study, in which growth response of chondrocytes and mesenchymal stem cells to this modified alginate will be monitored. Through this series of experiments, it will be possible to determine if binding peptide-modified alginate can act as a new scaffold material for *in vitro* cartilage tissue production.

2.1 Reagents and other chemicals

The following chemicals were used: ProNova UltraPure Low Viscosity Guluronate (UP LVG), a high G content alginate, was purchased from ProNova Biopolymers (Norway). Lyophilized human transforming growth factor-β1 (TGF- β1) and recombinant human insulin-like growth factor-I (IGF-I) were purchased from PeproTech (Rocky Hill, NJ). Trace tris hydroxymethylaminoethane buffer contaminants were removed from lyophilized TGF- β1 using a 5 kDa MWCO size-exclusion spin filter (Novagen). 11-amino-1-undecanethiol, hydrochloride (AUT; >99% purity) was purchased from Dojindo Laboratories (Kumamoto, Japan). Ethylenediamine was obtained from Aldrich Chemical Co. (Milwaukee, WI). All aqueous solutions were prepared using reagent grade deionized water.

The binding hexapeptides Glycine-Glycine-Tryptophan-Serine-Histidine-Tryptophan and Glycine-Glycine-Asparagine-Serine-Histidine-Asparagine, abbreviated with the single letter amino acid abbreviations GGWSHW and GGASHA, respectively, were produced by the Protein Core facilities at the University of Alabama at Birmingham. The peptide Glycine-Glycine-Glycine-Lysine(Dde)-Proline-Leucine-Histidine-Asparagine-Leucine-Leucine, abbreviated GGGKPLHALL, was purchased at 80% purity from Innovagen AB (Sweden). The additional 3 glycines at the N-terminus of this synthetic peptide sequence were added in order to provide a linker layer that would more fully expose the active peptides in the sequence once the peptide was bound to a surface. The lysine on this sequence was protected from unwanted chemical reactions by a Dde protecting group; this was removed using 5% hydrazine, anhydrous (Sigma) in dimethylformamide (DMF). Unless stated otherwise, all other chemicals were purchased from Sigma Chemical Co. (St. Louis, MO) and were used as received without further purification.

2.2 Chemical modification of alginate

In order to attach the binding peptides GGWSHW and KPLHALL to alginate, aqueous carbodiimide chemistry was utilized. Alginate chemistry was performed in 1% (w / v) UP LVG alginate solutions in 0.1 M MES buffer (pH 6.5, 0.3 M NaCl) for 20 hours. 1-ethyl-(dimethylaminopropyl) carbodiimide (EDC), a water-soluble carbodiimide, was used to form amide linkages between the amine group on the amino terminus of the peptide sequences and the carboxylate groups on the alginate polymer backbone.[33] The co-

reactant *N*-hydroxysulfosuccinimide (sulfo-NHS, Pierce, Rockford, IL) was used to stabilize the reactive EDC-intermediate against a competing hydrolysis reaction, raising the efficiency of amide bond formation,[34] and was dissolved in the alginate solution at a ratio of 1:2 to EDC.[35] 1 mg of synthesized peptide per gram alginate was added after 5 minutes of EDC activation.[36] The alginate product was purified by dialysis (3500 MWCO) against distilled H_2O for four days and lyophilized until dried.

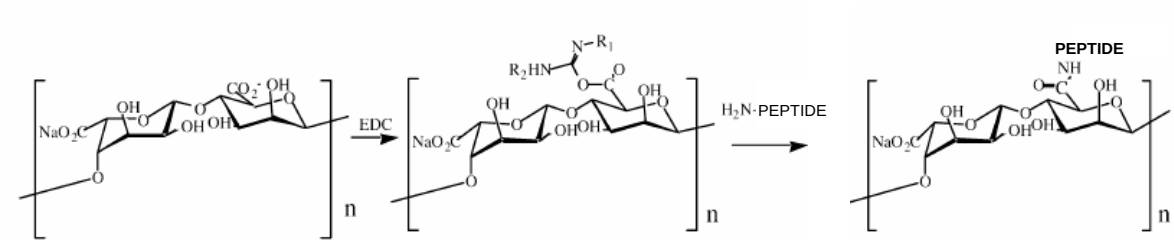

Figure 2.1. Covalent attachment of short peptides to alginate

2.3 Binding kinetics study

As outlined in the introduction of this thesis, the first aim of this project was to characterize the binding kinetics present between peptide-modified alginates and their respective growth factors. The non-covalent binding between free growth factor (GF_{Free}) and binding peptide (BP) can be formulated as:

$$GF_{Free} + BP \underset{k_{on}}{\overset{k_{off}}{\leftarrow \rightarrow}} GF_{Bound} \qquad \text{(Equation 1)}$$

The initial concentration of free growth factor is known; however, three experiments were undertaken to determine the binding constants k_{on} and k_{off}, as well as the concentration of GGWSHW or KPLHALL binding peptide covalently attached to alginate.

2.3.1 Imaging ellipsometry

In order to determine binding constants using surface plasmon resonance (section 2.3.2), the optimal chemistry to fabricate an alginate monolayer on a gold surface was determined using imaging ellipsometry.

Gold sensor chips for imaging ellipsometry and surface plasmon resonance studies were prepared by electronbeam evaporation of 1 nm of chromium followed by application of 50 nm of high-purity gold onto BK7 optical glass microscope slides obtained from Fischer Scientific (Pittsburg, PA). The glass slides were pre-cleaned with piranha solution for 30 min, rinsed, sonicated (5 min) in distilled H_2O, and then transferred to an evaporation setup. After metal evaporation, the substrates were sliced into 12.5 x 12.5 mm pieces with a diamond-tipped stylus and stored in a desiccator at room temperature. A second type of plain gold and carboxyl-terminated sensor chips, using SF10 glass, was purchased from Reichert Analytical Instruments (Reichert, Inc., Depew, NY). Before chemically modifying these gold surfaces, the blank SPR chips were cleaned with acetone and ethanol and rinsed in distilled H_2O.

Amino undecanethiol (AUT) self-assembled monolayers (SAMs) were formed on the gold surfaces by incubating the substrates in 1 mM ethanolic solutions of the thiol compound between 18 and 22 h (room temperature, no agitation). Although 10-12 hours usually is sufficient for chemiabsorption of thiol compounds onto gold surfaces, the longer incubation time was used to allow the molecular films to self-assemble into a crystalline-like solid phase.[37] Upon removal from the ethanol / thiol solution, the gold substrates were rinsed repeatedly in excess ethanol and blown dry using a stream of nitrogen gas. AUT SAM-modified substrates then were used immediately for fabrication of alginate sensor surfaces.

Gold surfaces with an AUT SAM were activated by incubating a 1% (w/v) solution of UP LVG alginate in a 10 mM solution of EDC / NHS in PBS (137 mM NaCl, 2.7 mM KCl, 4.3 mM $Na_2HPO_4 \cdot 7H_2O$, 1.4 mM KH_2PO_4, pH 7.2) for 5 minutes at room temperature. The EDC-activated alginate was incubated overnight on the AUT-modified gold surface. Subsequently, the substrates were washed with methanol to remove unbound alginate and blown dry with a stream of nitrogen gas.

To determine the binding efficiency to gold sensor chips, various concentrations of modified and unmodified alginate were bound to the gold surface using this new binding protocol and imaged using imaging ellipsometry (IE). The ellipsometric thickness of the AUT SAM and alginate layers assembled onto the gold substrates was estimated using a Nanofilm EP3 Imaging Ellipsometer. The chemistry

previously described for attachment of alginate to gold has, to our knowledge, never been performed; imaging ellipsometry quantified the amount of polymer bound to the surface, and thus the effectiveness of this new coupling procedure.

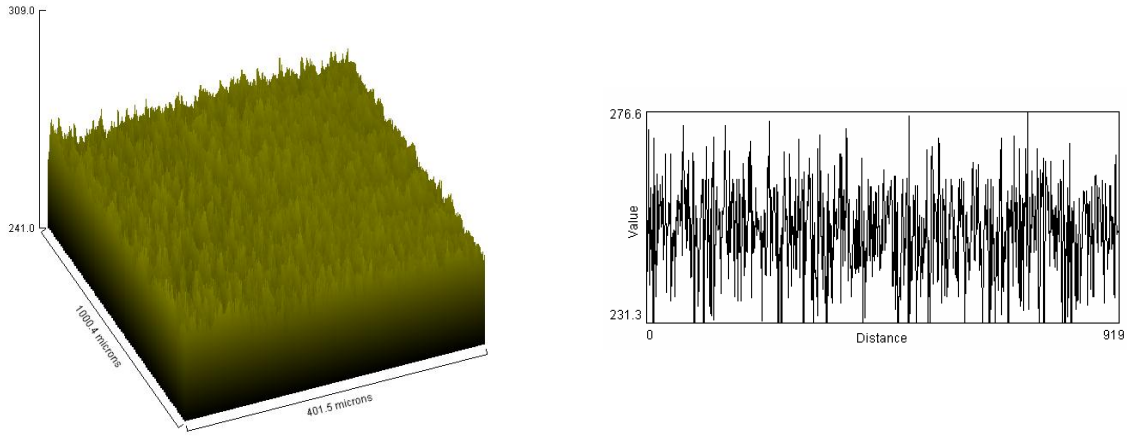

Figure 2.2. (Left) Imaging ellipsometry three-dimensional surface plot of alginate-modified surface; (Right) Variation in height of alginate across gold surface, in nm

Measurements were performed using multiple angles of incidence (70°, 65°, 60°) from 400 to 600 nm using a xenon arc lamp. Measurement at multiple angels generally improves confidence, as light travels different paths through the same film. The ellipsometric parameters δ and ψ were determined, which correlate with the thickness of alginate on the sensor surface and the chemical composition of the surface layers, respectively. The thickness of each layer immobilized on the SAM was estimated using theoretical modeling studies to fit the raw experimental data (δ and ψ), where δ shifts occur at approximately 1 degree per nanometer. Data such as that shown in Figure 2.2 above were obtained for varying concentration of unmodified alginate in the EDC / NHS reaction from 0.125% to 1.25% in order to determine the optimal concentration of alginate to immobilize for surface plasmon resonance experiments.

2.3.2 Surface plasmon resonance (SPR)

To determine the biospecific interaction and affinity of the binding of each growth factor to its respective binding peptide (i.e. k_{on} and k_{off}), a surface plasmon resonance (SPR) biosensor was used.

2.3.2.1 SPR background

As molecules are immobilized on the SPR sensor surface, the refractive index at the interface between the surface and a solution flowing over the surface changes, altering the angle at which reduced-intensity polarized light is reflected from the supporting glass plane.[38] The adsorption of biomolecules to the sensor surface results in a shift in the resonance angle, which is correlated with the refractive index of the solution flowing immediately adjacent to the gold-sensing surface; this change in angle is also proportional to the mass of bound material and is recorded in a sensorgram.

When sample is passed over the sensor surface, the sensorgram shows an increasing response as molecules associate. The response remains constant when the interaction reaches equilibrium. When sample is replaced by buffer, the response decreases as the interaction partners dissociate.[39] From these sensorgram profiles, kinetics (rates at which proteins interact) and affinity (how tightly binding peptides bind to the growth factor molecule) can be determined.

2.3.1.2 KPLHALL-IGF-I interaction

SPR measurements were performed on a model SR7000 Surface Plasmon Resonance Refractometer Instrument (Reichert, Inc., Depew, NY). For this SPR instrument, a change in one pixel report unit corresponded to a change in refractive index (RI) of approximately 10^{-6} RI. The change in pixel units as a function of time was monitored in real time using a LabView-based software program. Gold SPR sensor slides bound with modified and unmodified alginate were fabricated using chemistries that were characterized using imaging ellipsometry.

Typically, the biomolecular interaction experiments for IGF-I and alginate modified with GGGKPLHALL (25° C) were carried out in buffer for 10 minutes per sample, using a constant flow rate of 25 µl / min over the surface of the SPR chip. Concentrations of IGF-I ranged from 5 to 1000 nM. PBST (PBS plus 0.05% v/v Tween 20) was used as both the sample and flow buffer. After each binding experiment, the surface was regenerated with 40 mM HCl. The sensorgram profiles were analyzed using Scrubber 2 software

(BioLogic Software, Campbell, Australia). A representative sensorgram profile for this experiment is shown in Figure 2.3.

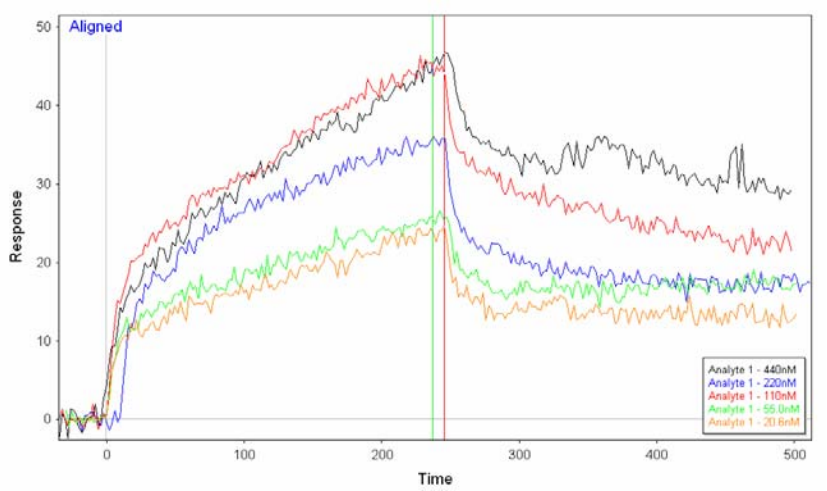

Figure 2.3. Aligned SPR kinetic curves for multiple concentrations of IGF-I used to evaluate binding strength to the synthetic peptide GGGKPLHALL.

2.3.2.3 GGWSHW-TGF-β1 interaction

Due to difficulties with the Reichert instrument, SPR measurements on TGF- β1 were performed using a different SPR instrument, a BIA2000 Surface Plasmon Resonance Instrument (BIAcore AB, Uppsala, Sweden). Due a difference in the sensor slides used for the SPR machines, CM5 carboxymethylated dextran chips and an ethylenediamine chemistry were used with the BIAcore system rather than AUT SAM-modified sensor slides. The biomolecular interaction experiments (25° C) were carried out in HBS buffer for 7 minutes per sample using a constant flow rate of 10 µl / min. Concentrations of TGF- β1 ranged from 10 to 1000 nM. After each binding experiment, the surface was regenerated with 40 mM HCl. Sensorgrams were generated and analyzed using BIAcore kinetic analysis software.

2.3.3 Attenuated total reflection Fourier transform infrared spectroscopy (ATR-FTIR)

To determine the density of binding peptides that were bound to the alginate (see Equation 1), and thus obtain more detailed information about the binding kinetics involved in this system, ATR-FTIR was

utilized. By creating a standard curve using known concentrations of binding peptide, one can quantitatively determine the approximate concentration of binding peptide in a sample of modified alginate. ATR-FTIR measurements were performed on a Vertex 80v FTIR spectrometer (Bruker Optics Inc., Billerica, MA) equipped with a germanium crystal-based ATR accessory unit. For each sample, a total of 16 scans were taken. Water was used to acquire the background spectrum. All spectra were collected in absorbance mode.

2.4 Controlled-release study

2.4.1 Computer-aided modeling

Using COMSOL Multiphysics Modeling Software version 1.1, Chemical Engineering Module (COMSOL Inc., Burlington, MA), a computational model for the diffusion of growth factor through alginate beads was created. Using this computer-aided calculation of transient mass transfer, the rate at which growth factor was released from growth factor-binding alginate beads seeded with growth factor could be predicted using the non-covalent reaction between free growth factor (GF_{Free}) and binding peptide (BP).

2.4.1.1 Governing equations

Three coupled reaction-diffusion equations were created to model diffusion kinetics of this system:

In alginate

$$\frac{\partial(GF_{Free})}{\partial t} = \left(D_{GF} \times \frac{1}{r^2} \times \frac{\partial}{\partial r} \left(r^2 \frac{\partial(GF_{Free})}{\partial r} \right) \right) - (kon \times BP \times GF_{Free}) + (koff \times GF_{Bound}) \quad \text{(Equation 2)}$$

$$\frac{\partial(GF_{Bound})}{\partial t} = (kon \times BP \times GF_{Free}) - (koff \times GF_{Bound}) \quad \text{(Equation 3)}$$

$$\frac{\partial(BP)}{\partial t} = -(kon \times BP \times GF_{Free}) + (koff \times GF_{Bound}) \quad \text{(Equation 4)}$$

In media

$$\frac{\partial(GF_{Free})}{\partial t} = \left(D_{GF} \times \frac{1}{r^2} \times \frac{\partial}{\partial r} \left(r^2 \frac{\partial(GF_{Free})}{\partial r} \right) \right) \quad \text{(Equation 5)}$$

2.4.1.1 Schematic & initial conditions

As diffusion is symmetric in all directions from the alginate bead, a one-dimensional model was created.

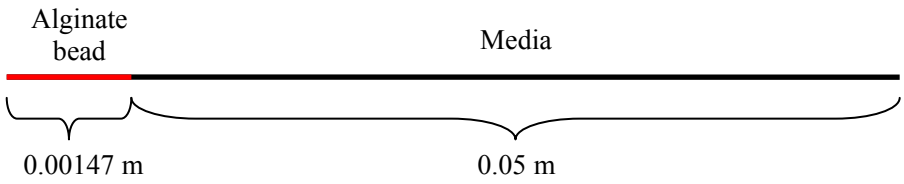

Figure 2.4. Schematic (not drawn to scale) of one-dimensional model representing diffusion of growth factor from an alginate bead into a semi-infinite media bath.

The radius of the media bath was progressively increased starting from 0.01 m until the free growth factor concentration in the alginate bead was found to be independent of the normal media surface radius. This radius was determined to be 0.05 m. A zero flux boundary condition could then be applied to the outer edge of the media: $\partial(GF_{Free})/\partial t = 0$. Concentration of growth factor was assumed to be continuous at the alginate-media interface.

Initially, the only species present are free growth factor, at $4.00 \times 10^{-7}\, mol/m^3$, and free binding peptides, at $0.1\, mg/g\ a\lg = 0.14\, mol/m^3$, both in the alginate. All other concentrations in all other regions are initially at zero. Binding constants k_{on} and k_{off} were varied from 10 to 100 m^3 / (mol sec) and 10^{-4} to 10^{-1} 1/sec, respectively. These binding constants are within the range obtained both through SPR and found in literature for other growth factor binding experiments. To determine average concentration for all time points, the following integration was performed for each time point for 288 locations within the model:

$$c_{a\lg inate,\ average} = \frac{\int 4\pi r^2 dr \times c}{(Total\ bead\ volume)}, \qquad \text{(Equation 6)}$$

where r is the linear coordinate along the horizontal axis of the model. Thus, controlled-release of growth factor from alginate beads was modeled. Using results from the computer model, an experimental controlled diffusion study was designed using alginate beads and ELISA.

2.4.2 Enzyme-linked ImmunoSorbent assay (ELISA)

In order to determine the functionality of this binding peptide-modified alginate in macro-scale situations, a controlled diffusion study was performed. To determine the kinetics of growth factor release from peptide-

modified alginate, growth factors were suspended in 2% peptide-modified alginate and analyzed for diffusion into the surrounding media. Unmodified LVG alginate beads acted as a control. Kinetic studies were performed using both human recombinant TGF-β1 and IGF-I. Peptide-modified alginate was diluted with Ultra Pure LVG alginate at 0.1 g TGF- β1 alginate: 1 g LVG alginate and 0.5 g IGF-I alginate: 1 g LVG alginate. Each growth factor was reconstituted in phosphate buffered saline with 0.1% BSA to a concentration of 10 ng TGF- β1 / ml PBS and 100 ng IGF-1 / ml PBS. The alginate was mixed with the reconstituted growth factor to create a 2% w/v (20 mg / ml) alginate solution. The alginate solution was sterile filtered using a 0.22 μm syringe filter.

Alginate beads were formed by dropping the prepared modified or unmodified alginate from a syringe (Becton-Dickson, Franklin Lakes, NJ) using a 22 gauge needle into a 102 mmol / L $CaCl_2$ solution (102 mM d-hydrous $CaCl_2$, 15 mM HEPES) for 10 minutes.[40] The beads were washed 3 times in 1 ml of sterile PBS to remove any growth factor that had not been incorporated into the bead. The beads were placed into 24-well culture dishes, each well containing 1 bead. The beads then were suspended in 1 ml of standard culture medium consisting of Dulbecco's Modified Eagle Medium (DMEM, high glucose) (Gibco, Invitrogen, Carlsbad, CA), 1% Insulin Transferrin Selenium (ITS), 0.1% Bovine Serum Albumin (BSA), 100 U / ml penicillin, and 100 μg / ml streptomycin.

The plates were maintained at 37° C in the tissue culture incubator. The medium was completely removed from the wells at five time points (2, 4, 8, 16, and 25 days), and replaced by fresh medium. An ELISA was used to measure the amount of growth factor that was released into the medium at various time points.

2.5 Cellular Study

To determine if covalent modification of alginate with binding peptides improves cell viability and ECM production, chondrocytes and mesenchymal stem cells (MSCs) were seeded in unmodified LVG alginate and binding peptide-modified alginate. Biochemical assays were utilized to determine the cellular effect of the modified-alginate scaffold.

2.5.1 Chondrocyte and MSC isolation and seeding

Bovine cartilage was harvested from the femoropatellar groove of 1-3-day-old calves. The harvested tissue was digested for 18 hours in Dulbecco's Modified Eagle Medium (DMEM) containing 3 mg /ml collagenase at 37°C and 5% CO_2. The digest was filtered with a 100 μm cell strainer (BD Bioscience, Bedford, MA) and then centrifuged at 412*g* for 7 minutes. The resulting cell pellet was washed twice with Dulbecco's phosphate-buffered saline (PBS) (Mediatech, Herndan, VA).

Bone marrow was aspirated from the iliac crest and sternum of euthanized horses from the Cornell University School of Veterinary Medicine. Red blood cells were lysed and the remaining nucleated cells were plated in tissue culture flasks to allow for adhesion of cell populations.[41] After 3 days, non-adherent cells were removed and the remaining cells were expanded for either 2 or 3 passages for seeding into alginate scaffolds.

Cell number for both cell types was determined using a hemocytometer (Hausser Scientific, Horsham, PA), and cell viability was determined using trypan blue dye. Chondrocytes and MSCs were then suspended into 10 mg / ml of LVG alginate or binding peptide modified-alginate at a seeding density of 6 x 10^7 cells / ml [42]. This cell-seeded alginate solution was cross-linked using the same alginate bead procedure as outlined in the ELISA section outlined in this thesis, with or without growth factor addition. Alginate beads were removed from culture at 0, 1, and 2 weeks and frozen at -80°C for biochemical analysis.

2.5.2 Biochemical analysis

Frozen samples were weighed on a microbalance and digested in 1 ml of 0.1 M sodium phosphate, 10 mM cysteine hydrochloride, and 3.8 U / ml papain at 60°C for 18 hours. Resulting biochemical contents were normalized to the wet weight of the sample.

2.5.2.1 Glycosaminoglycan (GAG) Assay

The glycosaminoglycan (GAG) content of the digests were measured as a marker for proteoglycans (key components of cartilage as discussed in the introduction of this thesis) using well-established methods.[43]

The assay was carried out in 96-well plates. In each well, 50 µl of digest was mixed with 250 µl of dye containing 16 mg / L 1,9-dimethylmethylene blue (DMMB) and 3.04 g / L glycine (pH 1.5). The absorbance was read at 595 nm using a microplate reader. Chondroitin-6-sulfate from shark cartilage was used to construct the standard curve.

2.5.2.2 DNA Assay

DNA content was measured as a marker of cell quantity (i.e. general cell proliferation and viability) using a Hoechst dye.[44] In each well, 190 µg / ml Hoechst 33258 dye in *tris*(hydroxymethyl)aminomethane EDTA saline (TES) buffer was added to 10 µl of the digested samples. Calf thymus DNA was used as a standard and DNA contents were determined by reaction with the Hoechst dye. Fluorescence was measured with an excitation wavelength at 348 nm and emission wavelength at 456 nm.

2.5.2.3 Hydroxyproline Assay

Hydroxyproline is a major ECM component that is specific to collagen. Therefore, hydroxyproline content was measured as a marker of collagen and ECM production. The hydroxyproline content of digests was measured using previously described methods.[45] 100 µl of each sample's digest was hydrolyzed in 100 µl of 2 N NaOH at 110°C for 18 hours. Afterwards, 20 µl 5N HCl, 100 µl 0.01 M $CuSO_4$, 100 µl 2.5 N NaOH, and 100 µl 6% H_2O_2 were added to the digested hydrolyzed sample in microfuge tubes. The tubes were allowed to sit at room temperature for 5 minutes, vortexed, and placed in a heat block at 80°C for 5 minutes. The tubes were then placed in an ice bath to cool to room temperature and 400 µl of 3N H_2SO_4 and 200 µl of 5 mg / ml p-dimethylaminobenzaldehyde in n-propanol (DMAB) were added to each tube. All assays were carried out in 96-well plates (Nalge Nunc, Rochester, NY). Each well of a 96-well plate was filled with 200 µl of a treated sample and absorbance was measured at 540 nm.

2.6 Statistics

Statistical analysis of biochemical data was completed using a two-way analysis of variance for chondrocytes data, and a t-test for MSC data ($p < 0.05$ for significance), using SAS Statistical Analysis System (SAS Institute, Cary, NC).

3.1 Binding kinetics study

3.1.1 Imaging Ellipsometry

The optical thickness of the AUT SAM was found to be 11.0 ± 2.0 Å for both the self-made and Reichert SPR chips; this falls within the range of ellipsometric thickness values that Mark et al. had observed previously.[37] The thickness measurement values suggest that a single monolayer of alginate was assembled on the gold substrates, confirming that successful derivatization of the gold sensor surface had occurred. The thickness of the layer of alginate, as measured by δ shifts, increased as the concentration of alginate used in the initial chemical procedure increased. The increase in Ψ with alginate concentration was not significant. The delta plot begins to plateau as the alginate concentration increases, demonstrating that the surface of the gold chip was approaching saturation with bound alginate, and steric hindrances due to repulsion of charged alginate monomers made a larger impact at these higher concentrations.

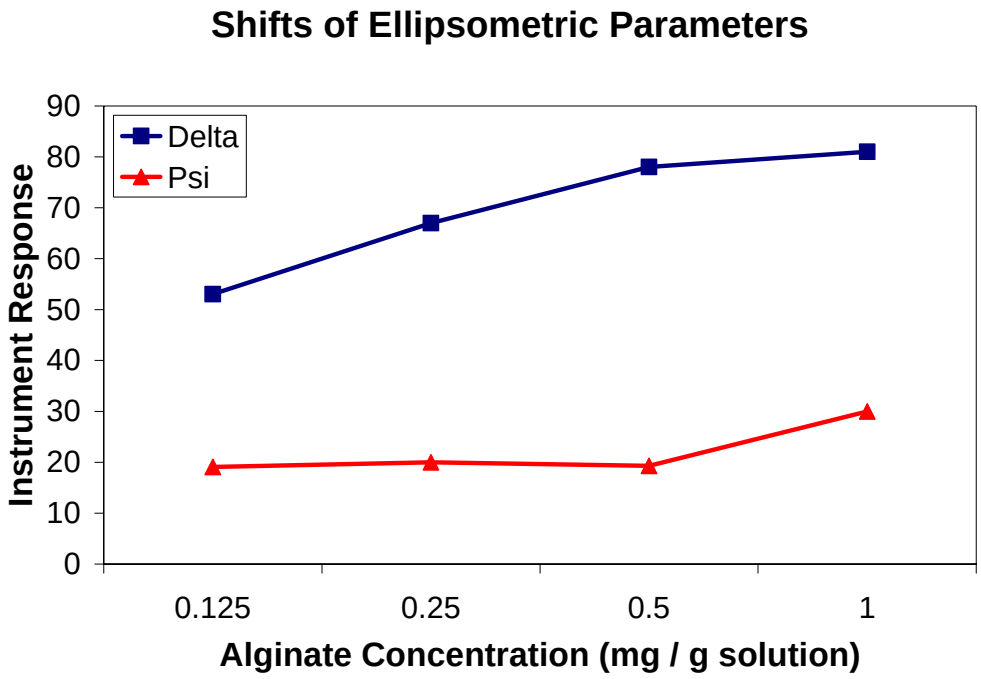

Figure 3.1. Measured shifts of the ellipsometric parameters delta and psi, which represent changes in thickness of surface layer and changes in chemical composition, respectively.

3.1.2 Surface Plasmon Resonance

3.1.2.1 KPLHALL-IGF-I interaction

Results were obtained using the Reichert SPR system to determine kinetic binding parameters between IGF-I and its respective binding peptide, GGGKPLHALL. The initial results suggest that the binding of this new IGF-I binding peptide was quite strong, with a range in overall dissociation constant typically between 50 nM and 2 μM.

k_{on} 1 / Ms	k_{off} 1 / s	K_D	Res SD
2.09E+05	1.98E-04	947.4 pM	1.216
52786.8	1.30E-03	24.55 nM	1.224
31179.5	1.52E-03	48.73 nM	1.458
12291.7	7.06E-04	57.44 nM	1.507
7941.7	1.00E-03	125.9 nM	3.425
5.4E+03	1.85E-3	340.0 nM	0.003
1181.1	1.53E-03	1.295 μM	0.811
912.8	1.62E-03	1.777 μM	1.477
33.78	4.79E-03	141.1 μM	2.244
3.926	1.00E-03	254.7 μM	2.308

Table 3.1. Compilation of representative SPR kinetics values for KPLHALL-modified alginate interaction with IGF-1.

However, in late fall 2006, it was determined that these SPR curves may have depicted considerably more binding than was actually present, due to non-specific binding within the Reichert SPR instrument. Qualitatively, however, a strong enhancement of signal intensity was obtained using the peptide-modified alginate surface, and the presence of the binding peptides on the alginate layer increased the amount of growth factor that was captured and retained on the sensor surface.

3.1.2.2 GGWSHW-TGF-β1 interaction

Results obtained from the BIAcore system on the GGWSHW-modified alginate (to bind TGF-β1) also show greater binding of growth factor to modified alginate than to unmodified alginate; however, quantitative determination of binding constants for this GGWSHW-TGF-β1 system was not accomplished.

3.1.3 ATR-FTIR

In the low-frequency regions of the IR spectra, the most informative features relevant for this study were the stretching and bending signals from amine and amide functional groups. The spectrum for the unmodified alginate shows only a weak relative absorption band centered at 1650 cm^{-1}, which is assigned to amide bending. The observation of stronger amide absorption bands in the modified alginate is consistent with the presence of surface-immobilized proteins. In the fingerprint region of the peptide sequence, there are two main features occurring at 1650 and 1540 cm^{-1} that are attributable to the amide I and II stretchings, respectively. Determination of density of binding peptides bound in modified alginate using this technique will be continued summer 2007 by other members of the laboratory. UV-VIS spectroscopy analysis showed an approximate concentration of 0.1 mg / g alginate for GGWSHW.

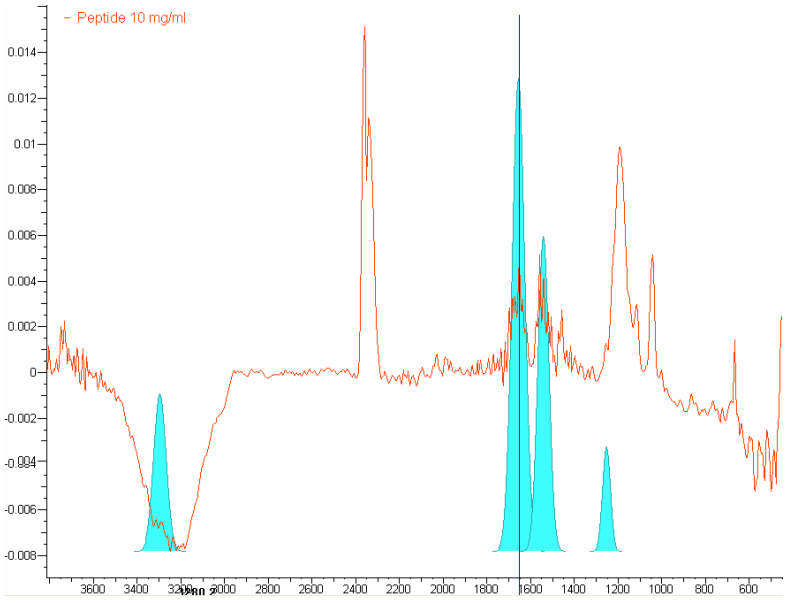

Figure 3.2. ATR-FTIR scan of GGGK(Dde)PLHALL peptide. Absorption bands occurring in the amide band regions of the IR spectra are shown in blue.

3.2 Controlled-release study

3.2.1 Computer-aided modeling

The following plots were generated using the COMSOL model:

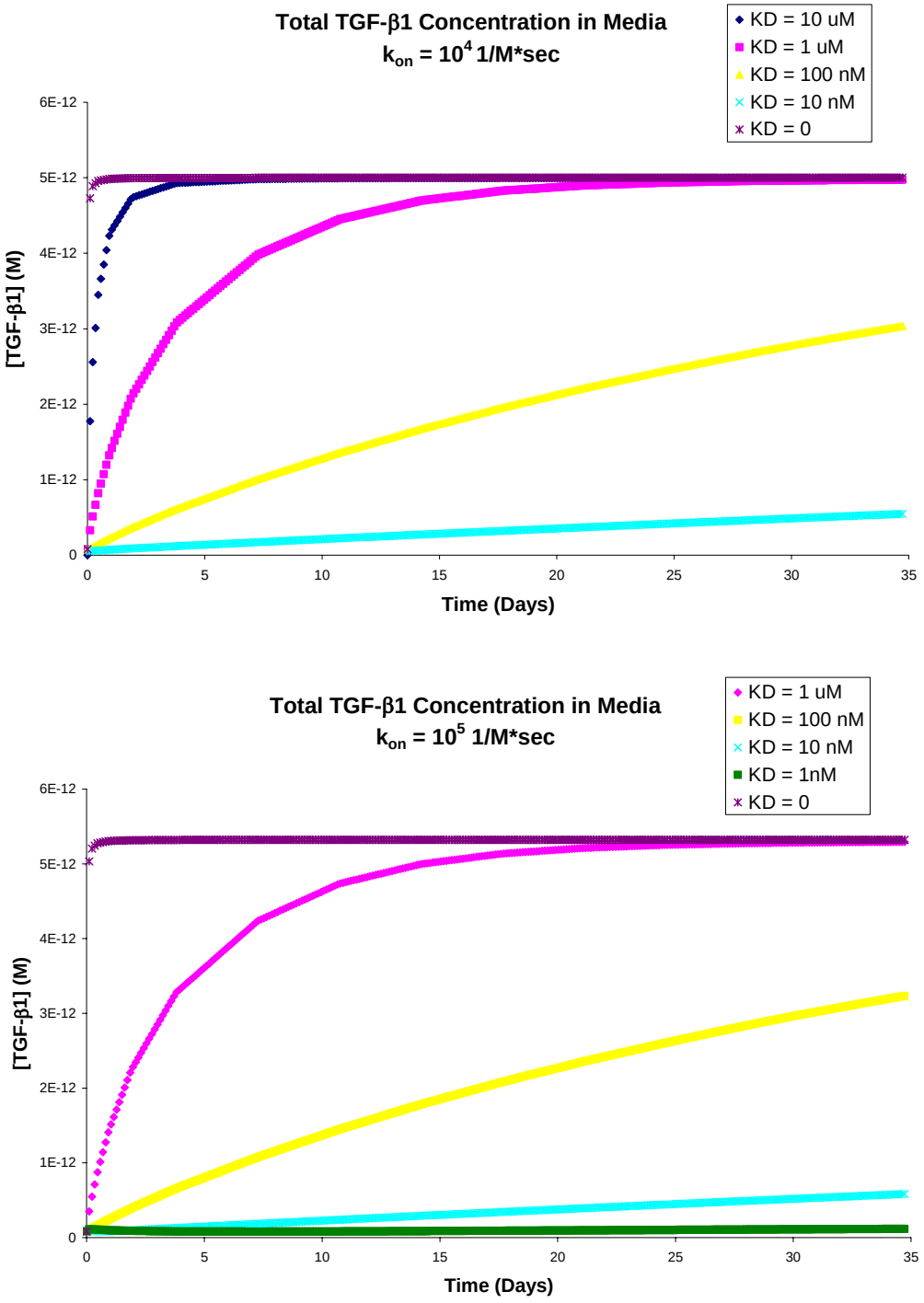

Figure 3.3, 3.4. Concentrations in media for various values of k_{on} and k_{off} for concentration of TGF-β1 in media.

For different k_{on} values, the diffusion profiles differed only slightly.

3.2.2 ELISA

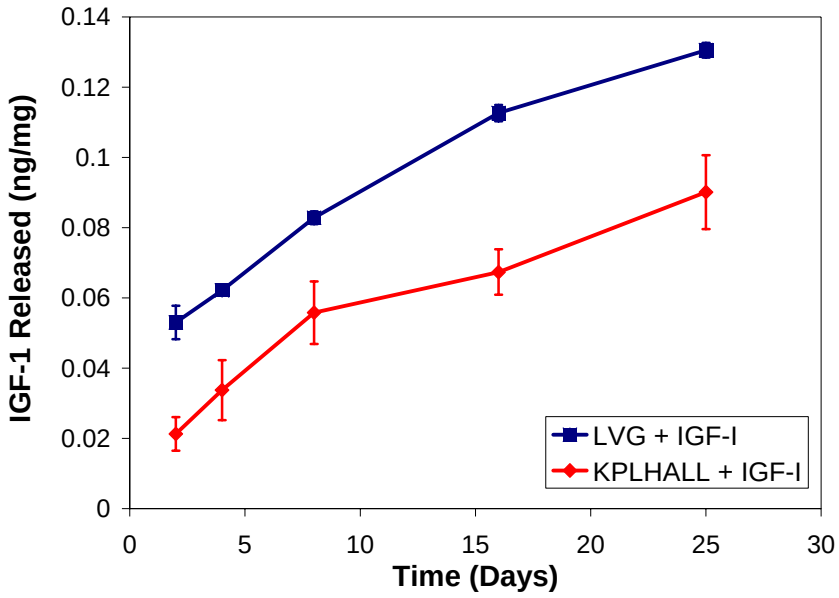

Figure 3.6. Release of IGF-I into media over time as determined by ELISA. Bath was collected at 2, 4, 8, 16, and 25 days (n = 3). Error bars are standard error of the mean for all graphs.

Because growth factors are non-covalently bound to their respective synthetic peptide on modified alginate beads, these beads show a markedly different concentration profile than beads composed of unmodified alginate.[46] Beads were 0.02 ml in volume with 2 ng total IGF-I per bead.

The ELISA for TGF-□1 was not able to detect growth factor release from either GGWSHW-modified or unmodified alginate beads. Lower growth factor seeding density (10 nM versus 100 nM for IGF-I-seeded beads) may have played a role. Additionally, transformation of TGF-□1 from latent to active form may have created experimental error leading to lack of signal.

3.3 Cellular study

3.3.1 GAG

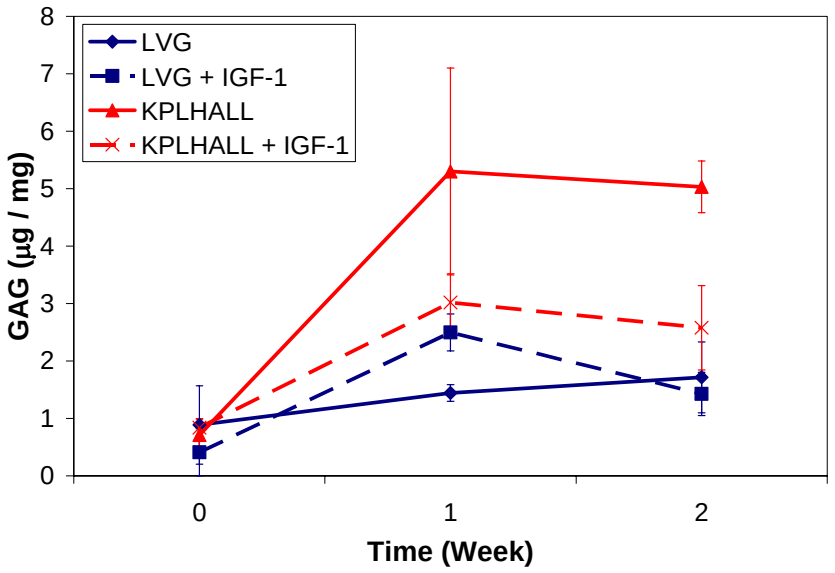

Figure 3.7. Total GAG content for chondrocytes, normalized by wet weight.

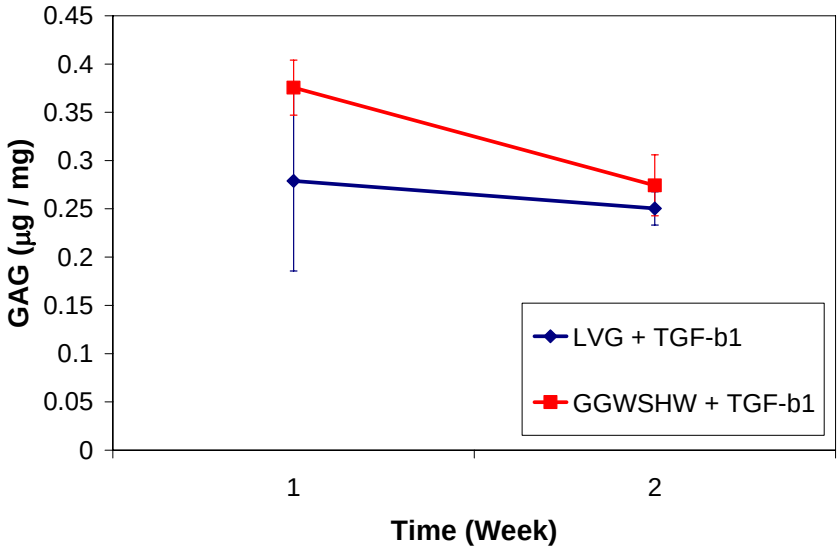

Figure 3.8 Total GAG content for MSCs, normalized by wet weight.

For chondrocytes, GAG content was found to be higher in week 1 ($p = 0.04$) and week 2 ($p = 0.01$) with KPLHALL than for LVG. Additionally, increase in GAG content from week 0 to week 2 was greater for KPLHALL than LVG ($p = 0.01$). A potentially confounding factor was that GAG content was lower in

week 2 with IGF-1 than for no growth factor addition (p = 0.03). Typically, one would expect IGF-I to increase cellular proliferation for both week 1 and week 2. The drop in week 2 may be due to an interaction between the alginate type and the growth factor treatment. Addition of IGF-1 reduced GAG with KPLHALL but had little effect on GAG with LVG (Interaction p = 0.03).

For MSCs, GAG content was higher in week 2 for GGWSHW than for LVG (p = 0.01), and the decrease in GAG content from week 1 to week 2 was greater for LVG than for GGWSHW (p = 0.01).

When one has an interaction, responses to main effects (either to IGF-1 addition or differences between KPLHALL alginate and LVG alginate) may be biased; in the presence of an interaction, one should exercise caution when interpreting main effects. Although there is an evident treatment interaction over time, changes in values over time are difficult to interpret, and changes later in time can be biased by changes earlier in time.

3.3.2 DNA

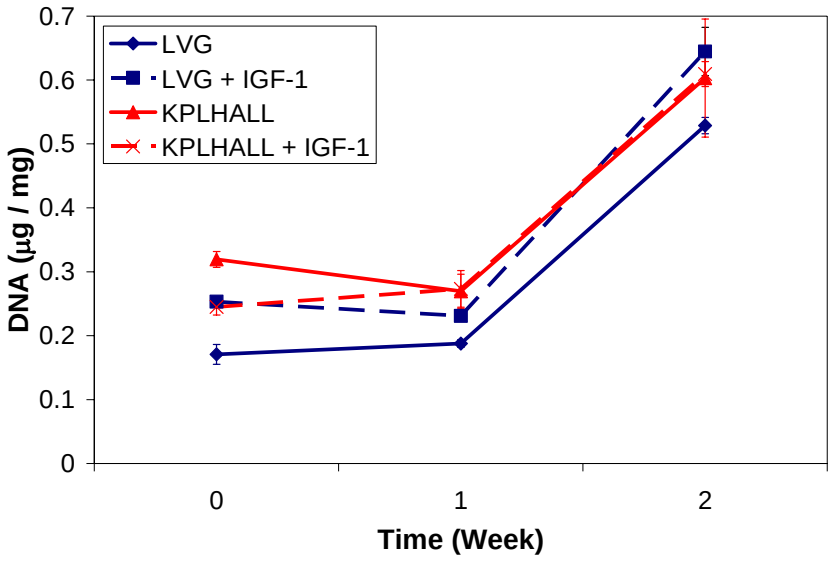

Figure 3.9. Total DNA content for chondrocytes, normalized by wet weight.

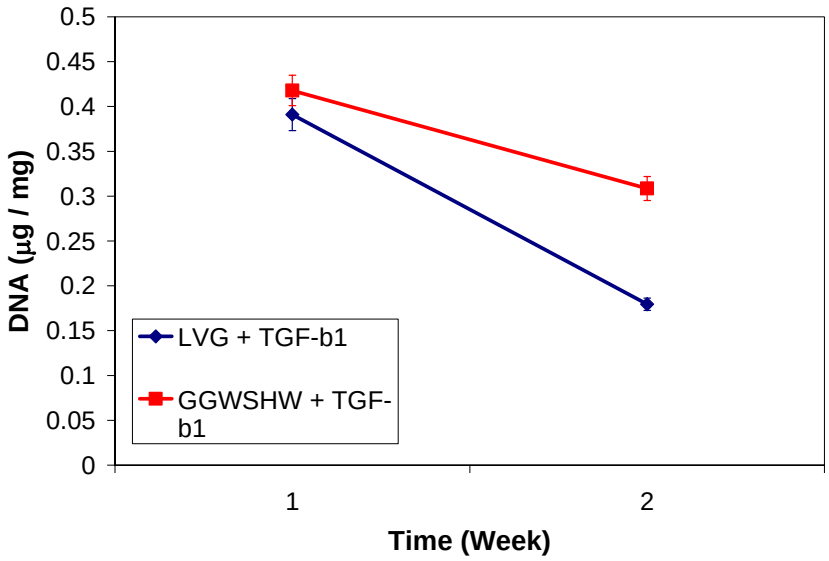

Figure 3.10. Total DNA content for MSCs, normalized by wet weight.

For chondrocytes, DNA content was higher in week 1 for KPLHALL than for LVG ($p = 0.01$). Adding IGF-1 to KPLHALL increased the degree of change in DNA from week 0 to week 1, but the addition of IGF-1 to LVG decreased this change over time (Interaction $p = 0.01$). Neither alginate type nor growth factor treatment made a significant difference in total DNA content for MSCs.

3.3.3 Hydroxyproline

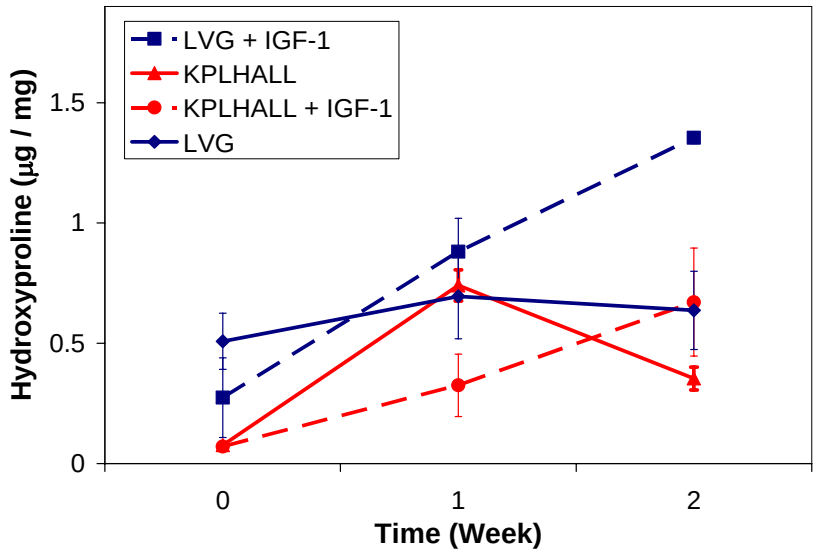

Figure 3.11. Total hydroxyproline content for chondrocytes, normalized by wet weight.

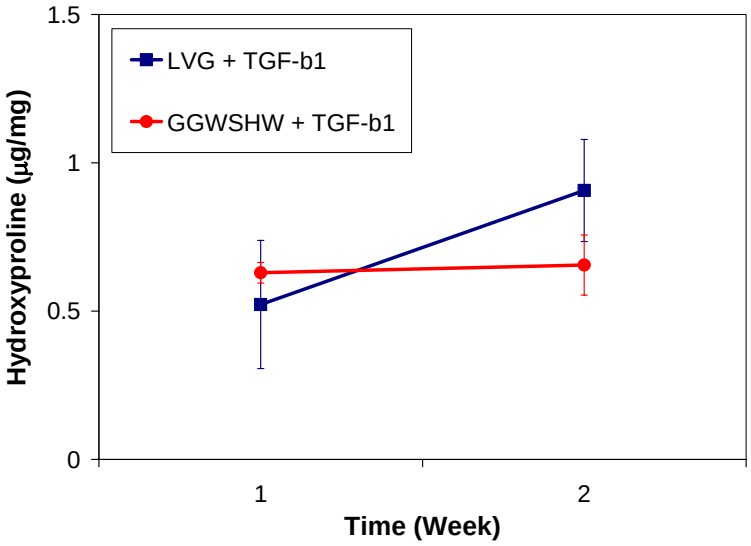

Figure 3.12. Total hydroxyproline content for MSCs, normalized by wet weight.

Hydroxyproline content increased significantly in modified alginate with growth factors ($p = 0.02$). Neither alginate type nor growth factor treatment made a significant difference in total DNA content for MSCs.

Using imaging ellipsometry and SPR, the binding constants between peptide-modified alginate and their respective growth factors was determined to be on the order of 100 nM to 1 μM. Comparing ELISA results to the modeling study, it appears that this level of binding is also present in IGF-1-modified alginate beads. The biochemical data demonstrates that binding peptide-modified alginate increases cell production of GAG, DNA, and hydroxyproline for certain time points.

The interaction between IGF-1 and the KPLHALL alginate response implies that response to IGF-1 addition differed depending on whether the cells received the KPL or the LVG treatment. Cells that were grown in KPLHALL-modified alginate without IGF-1 produced much more GAG than any other treatment class, suggesting that the IGF-1 produced by the chondrocytes is being bound by the modified-alginate and facilitating its growth.

As cells were only grown for a period of two weeks, long-term functional outcome is still a significant question. Future directions for research on this peptide-modified alginate system include continuation of ATR FT-IR studies, as well as repeating cell culture experiments with chondrocytes.

This work is the first step in creating and characterizing a synthetic ECM, using alginate as the base material, in which ligand type and density may be varied readily, and the cellular response specifically modified. In contrast to many previous systems, these alginate hydrogels may provide a practical system to transfer cell-material interaction studies into clinically relevant biomaterials. Alginate currently is being utilized in a number of trials to transplant multiple cell types and to treat biochemical or structural deficiencies; alginate matrices optimized for particular growth factor interactions may be readily used in these kinds of applications.

By incorporating specific growth factors within the alginate scaffold, without the adsorption of additional proteins that possibly could interfere with cellular behavior, cellular interactions can be characterized more thoroughly. For example, the IGF system plays a central role in many aspects of tumorigenesis. A better understanding of this complex system, which could be aided by alginate scaffolds that bind IGF-I, could

facilitate the development of novel approaches to diagnose and treat various human cancers and other diseases. Ultimately, the goal will be to produce a delivery system using growth factors, chondrocytes or mesenchymal stem cells, and a synthetic matrix of peptide-bound alginate to create a scaffold that can also be used to restore articular cartilage at minimal cost and patient morbidity. When placed in the correct combination and with the right mechanical stimuli, true restoration of articular cartilage may be ultimately achieved.

Author's Acknowledgments

The author would like to acknowledge Christopher Lee (Department of Material Science and Engineering) for his leadership and extensive work in the cellular study portion of this experiment. A more complete analysis of the biochemical assay data may be found in his senior thesis. Also, thanks to Nansen Yu (Department of Biological Engineering) and Magnus Bergvist for assistance with ATR-FTIR measurements. The author would also like to acknowledge Dr. Carl Batt (Department of Food Science) for use of his Reichert SPR; Tunde Babalola (Department of Biomedical Engineering) for harvest of MSCs; Dr. Moonsoo Jin, for his extremely helpful assistance with his BIAcore SPR, as well as discussions about experimental procedures. Finally, thanks to Dr. Lawrence Bonassar, for his constant support, guidance, and encouragement throughout this research project.

This work was supported by the Cornell Center for Materials Research (CCMR) with funding from the Materials Research Science and Engineering Center program of the National Science Foundation by the Cornell University Institute for Biotechnology and Life Science Technologies, a New York State Center for Advanced Technology supported by New York State and industrial partners. It was also supported by the Howard Hughes Medical Institute, Cornell University New Horizons Program by the Cornell School of Veterinary Medicine, and the Cornell University College of Agriculture and Life Science.

1. Langer, R. & Vacanti, J. P. Tissue engineering. *Science* **260**, 920-926 (1993).

2. Brittberg, M. *et al*. Treatment of deep cartilage defects in the knee with autologous chondrocyte transplantation. *N. Engl. J. Med.* **331**, 889-895 (1994).

3. Buckwalter, J. A., Saltzman, C. & Brown, T. The impact of osteoarthritis: implications for research. *Clin. Orthop. Relat. Res.* **(427 Suppl)**, S6-15 (2004).

4. Bonassar, L. J. in *Methods of Tissue Engineering* (eds Atala, A. & Lanza, R.) 1027-1039 (Academic Press, San Diego, 2002).

5. Mulliken, J. B. Repair of bilateral complete cleft lip and nasal deformity--state of the art. *Cleft Palate. Craniofac. J.* **37**, 342-347 (2000).

6. Tollefson, T. T. Advances in the treatment of microtia. *Curr. Opin. Otolaryngol. Head Neck Surg.* **14**, 412-422 (2006).

7. Ingber, D. E. & Folkman, J. Mechanochemical switching between growth and differentiation during fibroblast growth factor-stimulated angiogenesis in vitro: role of extracellular matrix. *J. Cell Biol.* **109**, 317-330 (1989).

8. Hardingham, T. E. & Fosang, A. J. Proteoglycans: many forms and many functions. *FASEB J.* **6**, 861-870 (1992).

9. Moreland, L. W. Intra-articular hyaluronan (hyaluronic acid) and hylans for the treatment of osteoarthritis: mechanisms of action. *Arthritis Res. Ther.* **5**, 54-67 (2003).

10. Ikada, Y. Challenges in tissue engineering. *J. R. Soc. Interface* **3**, 589-601 (2006).

11. Hunziker, E. B. Articular cartilage repair: basic science and clinical progress. A review of the current status and prospects. *Osteoarthritis Cartilage* **10**, 432-463 (2002).

12. Gilbert, J. E. Current treatment options for the restoration of articular cartilage. *Am. J. Knee Surg.* **11**, 42-46 (1998).

13. Minas, T. & Nehrer, S. Current concepts in the treatment of articular cartilage defects. *Orthopedics* **20**, 525-538 (1997).

14. Redman, S. N., Oldfield, S. F. & Archer, C. W. Current strategies for articular cartilage repair. *Eur. Cell. Mater.* **9**, 23-32; discussion 23-32 (2005).

15. Sohn, D. H. *et al*. Effect of gravity on localization of chondrocytes implanted in cartilage defects. *Clin. Orthop. Relat. Res.* **(394)**, 254-262 (2002).

16. Smetana, K.,Jr. Cell biology of hydrogels. *Biomaterials* **14**, 1046-1050 (1993).

17. Guo, J. F., Jourdian, G. W. & MacCallum, D. K. Culture and growth characteristics of chondrocytes encapsulated in alginate beads. *Connect. Tissue Res.* **19**, 277-297 (1989).

18. Jones, J. I. & Clemmons, D. R. Insulin-like growth factors and their binding proteins: biological actions. *Endocr. Rev.* **16**, 3-34 (1995).

19. Fortier, L. A., Mohammed, H. O., Lust, G. & Nixon, A. J. Insulin-like growth factor-I enhances cell-based repair of articular cartilage. *J. Bone Joint Surg. Br.* **84**, 276-288 (2002).

20. Baxter, R. C. Insulin-like growth factor binding proteins in the human circulation: a review. *Horm. Res.* **42**, 140-144 (1994).

21. Twigg, S. M., Kiefer, M. C., Zapf, J. & Baxter, R. C. Insulin-like growth factor-binding protein 5 complexes with the acid-labile subunit. Role of the carboxyl-terminal domain. *J. Biol. Chem.* **273**, 28791-28798 (1998).

22. Bach, L. A., Headey, S. J. & Norton, R. S. IGF-binding proteins--the pieces are falling into place. *Trends Endocrinol. Metab.* **16**, 228-234 (2005).

23. Kalus, W. *et al*. Structure of the IGF-binding domain of the insulin-like growth factor-binding protein-5 (IGFBP-5): implications for IGF and IGF-I receptor interactions. *EMBO J.* **17**, 6558-6572 (1998).

24. Thompson, J. D., Higgins, D. G. & Gibson, T. J. CLUSTAL W: improving the sensitivity of progressive multiple sequence alignment through sequence weighting, position-specific gap penalties and weight matrix choice. *Nucleic Acids Res.* **22**, 4673-4680 (1994).

25. Imai, Y. *et al*. Substitutions for hydrophobic amino acids in the N-terminal domains of IGFBP-3 and -5 markedly reduce IGF-I binding and alter their biologic actions. *J. Biol. Chem.* **275**, 18188-18194 (2000).

26. Young, G. D. & Murphy-Ullrich, J. E. Molecular interactions that confer latency to transforming growth factor-beta. *J. Biol. Chem.* **279**, 38032-38039 (2004).

27. Daniel, C. *et al*. Thrombospondin-1 is a major activator of TGF-beta in fibrotic renal disease in the rat in vivo. *Kidney Int.* **65**, 459-468 (2004).

28. Ievdokymova, N. I. & Komisarenko, S. V. Thrombospondin-1-dependent mechanism of transforming growth factor beta-1 activation in cultured human endothelial cells. *Ukr. Biokhim. Zh.* **76**, 83-89 (2004).

29. Ribeiro, S. M., Poczatek, M., Schultz-Cherry, S., Villain, M. & Murphy-Ullrich, J. E. The activation sequence of thrombospondin-1 interacts with the latency-associated peptide to regulate activation of latent transforming growth factor-beta. *J. Biol. Chem.* **274**, 13586-13593 (1999).

30. Yevdokimova, N., Wahab, N. A. & Mason, R. M. Thrombospondin-1 is the key activator of TGF-beta1 in human mesangial cells exposed to high glucose. *J. Am. Soc. Nephrol.* **12**, 703-712 (2001).

31. Schultz-Cherry, S. *et al*. Regulation of transforming growth factor-beta activation by discrete sequences of thrombospondin 1. *J. Biol. Chem.* **270**, 7304-7310 (1995).

32. Murphy-Ullrich, J. E. & Poczatek, M. Activation of latent TGF-beta by thrombospondin-1: mechanisms and physiology. *Cytokine Growth Factor Rev.* **11**, 59-69 (2000).

33. Grabarek, Z. & Gergely, J. Zero-length crosslinking procedure with the use of active esters. *Anal. Biochem.* **185**, 131-135 (1990).

34. Staros, J. V., Wright, R. W. & Swingle, D. M. Enhancement by N-hydroxysulfosuccinimide of water-soluble carbodiimide-mediated coupling reactions. *Anal. Biochem.* **156**, 220-222 (1986).

35. Genes, N. G., Rowley, J. A., Mooney, D. J. & Bonassar, L. J. Effect of substrate mechanics on chondrocyte adhesion to modified alginate surfaces. *Arch. Biochem. Biophys.* **422**, 161-167 (2004).

36. Rowley, J. A., Madlambayan, G. & Mooney, D. J. Alginate hydrogels as synthetic extracellular matrix materials. *Biomaterials* **20**, 45-53 (1999).

37. Mark, S. S., Sandhyarani, N., Zhu, C., Campagnolo, C. & Batt, C. A. Dendrimer-functionalized self-assembled monolayers as a surface plasmon resonance sensor surface. *Langmuir* **20**, 6808-6817 (2004).

38. Johnsson, B., Lofas, S. & Lindquist, G. Immobilization of proteins to a carboxymethyldextran-modified gold surface for biospecific interaction analysis in surface plasmon resonance sensors. *Anal. Biochem.* **198**, 268-277 (1991).

39. Lahiri, J., Isaacs, L., Tien, J. & Whitesides, G. M. A strategy for the generation of surfaces presenting ligands for studies of binding based on an active ester as a common reactive intermediate: a surface plasmon resonance study. *Anal. Chem.* **71**, 777-790 (1999).

40. Masuda, K., Sah, R. L., Hejna, M. J. & Thonar, E. J. A novel two-step method for the formation of tissue-engineered cartilage by mature bovine chondrocytes: the alginate-recovered-chondrocyte (ARC) method. *J. Orthop. Res.* **21**, 139-148 (2003).

41. Fortier, L. A., Nixon, A. J., Williams, J. & Cable, C. S. Isolation and chondrocytic differentiation of equine bone marrow-derived mesenchymal stem cells. *Am. J. Vet. Res.* **59**, 1182-1187 (1998).

42. Lee, C. S. *et al*. Integration of layered chondrocyte-seeded alginate hydrogel scaffolds. *Biomaterials* **28**, 2987-2993 (2007).

43. Enobakhare, B. O., Bader, D. L. & Lee, D. A. Quantification of sulfated glycosaminoglycans in chondrocyte/alginate cultures, by use of 1,9-dimethylmethylene blue. *Anal. Biochem.* **243**, 189-191 (1996).

44. Kim, Y. J., Sah, R. L., Doong, J. Y. & Grodzinsky, A. J. Fluorometric assay of DNA in cartilage explants using Hoechst 33258. *Anal. Biochem.* **174**, 168-176 (1988).

45. NEUMAN, R. E. & LOGAN, M. A. The determination of hydroxyproline. *J. Biol. Chem.* **184**, 299-306 (1950).

46. Mierisch, C. M. *et al*. Transforming growth factor-beta in calcium alginate beads for the treatment of articular cartilage defects in the rabbit. *Arthroscopy* **18**, 892-900 (2002).